Structure, Vol. 12, 1471–1480, August, 2004, ©2004 Elsevier Ltd. All rights reserved. DOI 10.1016/j.str.2004.05.020

Crystal Structure of the Native Chaperonin Complex from *Thermus thermophilus* Revealed Unexpected Asymmetry at the *cis*-Cavity

Tatsuro Shimamura,[1] Ayumi Koike-Takeshita,[2] Ken Yokoyama,[3] Ryoji Masui,[4] Noriyuki Murai,[2,7] Masasuke Yoshida,[2,3] Hideki Taguchi,[2,5,8,*] and So Iwata[1,3,6,*]

[1]Department of Biological Sciences
Imperial College London
London SW7 2AZ
United Kingdom

[2]Chemical Resources Laboratory
Tokyo Institute of Technology
Yokohama 226-8503
Japan

[3]ATP System Project
Exploratory Research for Advanced Technology (ERATO)
Japan Science and Technology Agency
Yokohama 226-0026
Japan

[4]Graduate School of Science
Osaka University
Toyonaka, Osaka 560-0063
Japan

[5]Precursory Research for Embryonic Science and Technology (PRESTO)
Japan Science and Technology Agency
4-1-8 Honcho, Kawaguchi
Saitama, 332-0012
Japan

[6]Division of Biomedical Sciences
Imperial College London
London SW7 2AZ
United Kingdom

Summary

The chaperonins GroEL and GroES are essential mediators of protein folding. GroEL binds nonnative protein, ATP, and GroES, generating a ternary complex in which protein folding occurs within the cavity capped by GroES (*cis*-cavity). We determined the crystal structure of the native GroEL-GroES-ADP homolog from *Thermus thermophilus*, with substrate proteins in the *cis*-cavity, at 2.8 Å resolution. Twenty-four in vivo substrate proteins within the *cis*-cavity were identified from the crystals. The structure around the *cis*-cavity, which encapsulates substrate proteins, shows significant differences from that observed for the substrate-free *Escherichia coli* GroEL-GroES complex. The apical domain around the *cis*-cavity of the *Thermus* GroEL-GroES complex exhibits a large deviation from the 7-fold symmetry. As a result, the GroEL-GroES interface differs considerably from the previously reported *E. coli* GroEL-GroES complex, including a previously unknown contact between GroEL and GroES.

*Correspondence: taguchi@k.u-tokyo.ac.jp (H.T.); s.iwata@ic.ac.uk (S.I.)

[7]Present address: Second Department of Biochemistry, Jikei University School of Medicine, 3-25-8 Nishi-shinbashi, Minato-ku, Tokyo 105-8461, Japan.

[8]Present address: Department of Medical Genome Sciences, Graduate School of Frontier Sciences, The University of Tokyo, Kashiwa, Chiba 277-8562, Japan.

Introduction

Chaperonins are essential proteins that mediate the folding of newly translated polypeptides in an ATP-dependent manner (Bukau and Horwich, 1998; Hartl and Hayer-Hartl, 2002; Sigler et al., 1998; Thirumalai and Lorimer, 2001). In eubacteria, mitochondria, and chloroplasts, two ring-shaped chaperonins, GroEL (cpn60) and the co-chaperonin GroES (cpn10), act together. GroEL from *Escherichia coli* (*Ec*-GroEL) is the best-characterized chaperonin and comprises two heptameric rings stacked back to back, each containing seven identical 57 kDa subunits (Braig et al., 1994, 1995). *Ec*-GroEL has three domains: an equatorial domain containing an ATP/ADP binding site, an apical domain with the binding site for both nonnative proteins and GroES, and an intermediate domain that has a hinge region connecting the equatorial and the apical domains (Braig et al., 1994). *E. coli* GroES (*Ec*-GroES) is a dome-shaped structure containing seven identical 10 kDa subunits that binds to one of the *Ec*-GroEL rings (Hunt et al., 1996).

GroEL binds a wide spectrum of nonnative proteins at hydrophobic sites on the apical domains (Fenton et al., 1994; Houry et al., 1999; Sakikawa et al., 1999; Viitanen et al., 1992). Binding of ATP to one of the GroEL rings induces a positive cooperative upward movement of the intermediate and apical domains, leading to stable binding of GroES (Xu et al., 1997). Negative cooperativity between the two GroEL rings with respect to ATP binding (Yifrach and Horovitz, 1995) results in an asymmetric GroEL-GroES (GroEL/ES) complex, in which the GroEL ring that binds GroES is referred to as the *cis*-ring and the opposite ring as the *trans*-ring. The majority of GroEL residues involved in GroES binding are also involved in binding nonnative protein (Fenton et al., 1994). As a result, GroES binding encapsulates the nonnative protein within the enlarged cavity inside the *cis*-ring capped by the dome of GroES (the *cis*-cavity) (Mayhew et al., 1996; Weissman et al., 1995). The nonnative protein inside the cavity initiates folding to the native state without risk of aggregation (referred to as *cis*-folding). After ATP hydrolysis in the *cis*-ring, the subsequent binding of ATP to the *trans*-ring triggers the release of GroES, ADP, and the folded or partially folded substrate protein from the *cis*-ring (Rye et al., 1997, 1999).

The structure of the GroEL-GroES-ADP_7 complex from *E. coli* (Xu et al., 1997) has revealed important features of the complex: the large en bloc movement of the intermediate and apical domains in the *cis*-ring, the enlarged *cis*-cavity, the hydrophilic surface of the *cis*-cavity, and the binding of the mobile loop in GroES to helices H and I of GroEL. However, this *Ec*-GroEL/ES complex

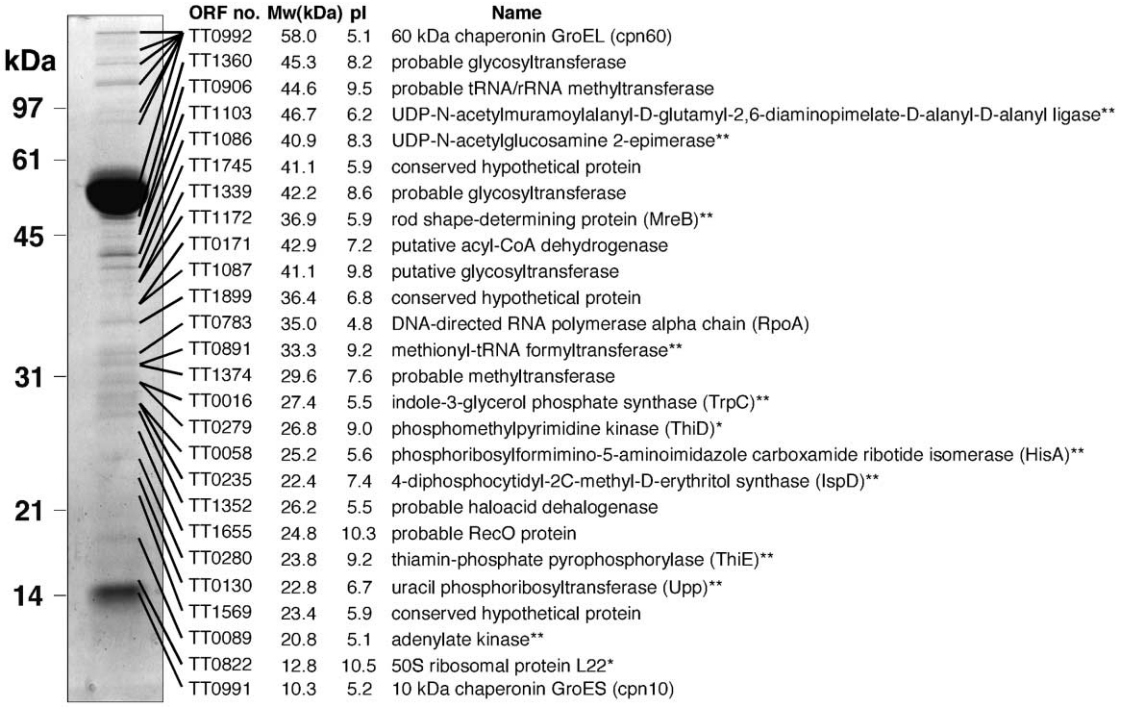

ORF no.	Mw(kDa)	pI	Name
TT0992	58.0	5.1	60 kDa chaperonin GroEL (cpn60)
TT1360	45.3	8.2	probable glycosyltransferase
TT0906	44.6	9.5	probable tRNA/rRNA methyltransferase
TT1103	46.7	6.2	UDP-N-acetylmuramoylalanyl-D-glutamyl-2,6-diaminopimelate-D-alanyl-D-alanyl ligase**
TT1086	40.9	8.3	UDP-N-acetylglucosamine 2-epimerase**
TT1745	41.1	5.9	conserved hypothetical protein
TT1339	42.2	8.6	probable glycosyltransferase
TT1172	36.9	5.9	rod shape-determining protein (MreB)**
TT0171	42.9	7.2	putative acyl-CoA dehydrogenase
TT1087	41.1	9.8	putative glycosyltransferase
TT1899	36.4	6.8	conserved hypothetical protein
TT0783	35.0	4.8	DNA-directed RNA polymerase alpha chain (RpoA)
TT0891	33.3	9.2	methionyl-tRNA formyltransferase**
TT1374	29.6	7.6	probable methyltransferase
TT0016	27.4	5.5	indole-3-glycerol phosphate synthase (TrpC)**
TT0279	26.8	9.0	phosphomethylpyrimidine kinase (ThiD)*
TT0058	25.2	5.6	phosphoribosylformimino-5-aminoimidazole carboxamide ribotide isomerase (HisA)**
TT0235	22.4	7.4	4-diphosphocytidyl-2C-methyl-D-erythritol synthase (IspD)**
TT1352	26.2	5.5	probable haloacid dehalogenase
TT1655	24.8	10.3	probable RecO protein
TT0280	23.8	9.2	thiamin-phosphate pyrophosphorylase (ThiE)**
TT0130	22.8	6.7	uracil phosphoribosyltransferase (Upp)**
TT1569	23.4	5.9	conserved hypothetical protein
TT0089	20.8	5.1	adenylate kinase**
TT0822	12.8	10.5	50S ribosomal protein L22*
TT0991	10.3	5.2	10 kDa chaperonin GroES (cpn10)

Figure 1. Substrate Proteins of the Native *Tth*-Chaperonin Complex Obtained from Crystals

A 1D gel of the crystals is shown with a list of 24 identified substrate proteins as well as *Tth*-GroEL and *Tth*-GroES. A star denotes substrate proteins of known structure. A double star denotes substrate proteins which have a homolog of known structure.

was obtained by reconstitution of individually purified *Ec*-GroEL and *Ec*-GroES with ADP. Dissociation of *Ec*-GroEL and *Ec*-GroES during purification prevented isolation of the native *Ec*-GroEL/ES complex. As a result, this complex contains no substrate protein and thus may not represent any real intermediates in the GroEL-ATPase cycle. Indeed, an exclusive role for ATP (not ADP) in productive *cis*-folding has been reported (Chaudhry et al., 2003; Motojima and Yoshida, 2003), suggesting a different conformation for GroEL when the reaction is initiated by ATP from that observed in the *Ec*-GroEL/ES complex. The following findings also suggest there are some interactions between the *cis*-cavity and the substrate proteins during the catalytic cycle of the GroEL/ES complex; (i) the GroEL-ATPase cycle is accelerated several fold in the presence of nonnative proteins (Yifrach and Horovitz, 1996; Rye et al., 1999; Aoki et al., 2000, Taguchi et al., 2001). (ii) It has been proposed that GroEL forces the unfolding of substrate proteins in a GroES- and ATP-dependent manner (Shtilerman et al., 1999). (iii) Folding of some proteins in the *cis*-cavity is faster than spontaneous folding in bulk solution (Brinker et al., 2001). (iv) Changing the surface of the *cis*-cavity wall from hydrophobic to hydrophilic affects protein folding (Wang et al., 2002). To understand the interaction between the *cis*-cavity and substrate proteins, it is essential to obtain the structure of the GroEL-GroES-substrate complex.

In this paper, we report the crystal structure of the native chaperonin complex from *Thermus thermophilus* (*Tth*), an eubacterial homolog of *E. coli* chaperonin (*Ec*-GroEL/ES) complex. We identified 24 substrate proteins among those encapsulated inside the *Tth*-chaperonin complex. Moreover, a comparative study with the reconstituted *Ec*-GroEL/ES complex reveals significant differences between the two protein complexes, particularly around the *cis*-cavity, where substrate protein is encapsulated.

Results and Discussion

Identification of In Vivo Substrate Proteins

The *Tth*-chaperonin complex was purified in buffer containing no nucleotides to avoid exchange of *Tth*-GroES (Shimamura et al., 2003; Taguchi et al., 1991; Taguchi and Yoshida, 1998). In addition, the buffer contained Triton X-100, which has been shown to remove the polypeptides bound to the *trans*-ring of the *Tth*-chaperonin complex (data not shown). The addition of Triton X-100 does not affect the stability of the complex. The *Tth*-chaperonin complex crystals were solubilized and the proteins separated by SDS-PAGE. In addition to the strong bands corresponding to *Tth*-GroEL (~58 kDa) and *Tth*-GroES (~11 kDa), there were many faint bands observable on the gel (Figure 1). Using MALDI-TOF mass spectrometry and Edman degradation, we succeeded in identifying 24 of the most abundant proteins (Figure 1). This analysis also revealed that all bands larger than 58 kDa are likely to be aggregated and/or crosslinked GroEL.

The list of identified proteins reveals no sequence nor motif similarity, as well as no preference for pI. Only three (Upp, ThiD, and RpoA) have so far been known to be *Ec*-GroEL-interacting proteins (Houry et al., 1999) and

Table 1. Data Collection and Refinement Statistics

Data Collection	
Wavelength (Å)	0.933
Resolution (Å)	2.8
Measured reflections	647,041
Unique reflections	429,625
Completeness (%)[a]	81.3 (65.9)[b]
R_{merge} (%)[c]	7.6 (55.5)
Space group	*P*1
Unit cell (Å)	a = 140.4, b = 156.4, c = 273.2 α = 82.9°, β = 85.4°, γ = 68.5°
Refinement	
Resolution (Å)	40–2.8 (2.9–2.8)
R_{work} (%)[d]	23.9 (40.5)
R_{free} (%)[e]	27.9 (37.6)
Rmsd from ideal value	
Bond lengths (Å)	0.008
Bond angles (°)	1.23
Dihedral angles (°)	20.5
Improper torsion angles (°)	0.77
Ramachandran statistics	
Most favored region (%)	85.7
Additional allowed region (%)	14.0
Generously allowed region (%)	0.0
Disallowed region (%)	0.2

[a] Values in parentheses are for the highest resolution shell.
[b] Due to strong anisotropy, the completeness of the last shell R_{merge} is low.
[c] $R_{merge} = \Sigma_i |I(h)_i - /\Sigma_i |I(h)_i|$, where is the mean intensity of equivalent reflections.
[d] $R_{work} = \Sigma|F_o - F_c|/\Sigma|F_o|$, where F_o and F_c are the observed and calculated structure factor amplitudes, respectively.
[e] $R_{free} = \Sigma|F_o - F_c|/\Sigma|F_o|$, calculated using a test data set, 3% of total data randomly selected from the observed reflections.

Tth-chaperonin substrate proteins. Among the identified proteins, the structures of ThiD and the 50S ribosomal protein L22 have been solved. In addition, the structures of ten homologous proteins (more than 30% sequence identity) from different bacteria have been solved. All of them contain α/β folds as suggested for *Ec*-GroEL-interacting proteins (Houry et al., 1999), although this is a very common structural feature. As we have many bands corresponding to shown proteins as well as the 24 substrate proteins shown here, we await further analysis in order to fully elucidate common structural features among chaperonin substrates.

Overall Structure of the *T. thermophilus* Chaperonin-Substrate Complex

The structure was determined at 2.8 Å resolution (Table 1). Because of the averaging using the 14-fold NCS, electron density was clear in most regions including the side chains. The overall structure of the *Tth*-chaperonin complex is similar to the *Ec*-GroEL/ES complex (Figure 2A), reflecting the high sequence similarity (64% for GroES and 71% for GroEL) (Figure 3). This complex binds seven ADP molecules to the *cis*-ring but not to the *trans*-ring (Figure 2A). The structures of individual subunit and domain are also similar, with root-mean-square deviations (rmsd) of Cα atoms of 0.7–1.2 Å (domains) and 1.1–1.6 Å (subunits), except for the GroES mobile loop (rmsd 3.0 Å), the binding region to GroEL. There are 13 nonconserved regions (I–XIII in Figure 3) between the *Ec*-GroEL/ES and *Tth*-chaperonin complex sequences. Except regions III and XIII, all these nonconserved regions are located on the outside of the central cavity (Figure 2B). In contrast, residues facing the *cis*-cavity are highly conserved and mainly charged (Figure 3). These residues are also conserved in other chaperonins (data not shown), suggesting that the location of these residues could be important for the efficient folding of the substrate in addition to the previously suggested role of maintaining the hydrophilicity of the wall (Xu et al., 1997). Interestingly, the inside surface of the *cis*-cavity is very acidic (Figure 2C).

Although biochemical analysis clearly showed the presence of substrate protein in the *cis*-cavity, we could only observe very disordered electron densities on the surface of the *cis*-cavity. This is expected, as, in the crystal structure, we are observing an averaged electron density distribution of more than 24 different substrate proteins. Despite this, it is still possible to observe a general effect of the substrate in the *cis*-cavity to the *Tth*-chaperonin complex structure, which will be discussed in the following sections.

The *cis*-Ring

GroES and the GroEL *cis*-ring form the large *cis*-cavity for the encapsulation of substrate proteins. In spite of the similarity of the structures of each subunit and domain, the overall shape of the *cis*-ring rim in the *Tth*-chaperonin complex, composed of the apical domains, is strikingly different from the *Ec*-GroEL/ES complex (Figure 4A). The shape of the *cis*-ring rim in the *Ec*-GroEL/ES complex is almost circular, whereas the rim of the *Tth*-chaperonin complex has an irregular oval shape deviating from the molecule's 7-fold symmetry. Both molecules in an asymmetric unit show similar deviation from 7-fold symmetry (Figure 4A). Such large deviation from 7-fold symmetry is observed only in the apical domains of the *cis*-ring but not in other parts of the molecule. This deviation of the *cis*-ring rim from the 7-fold symmetry is not a direct effect of the crystal contact because the same distortion pattern of the ring is observed for both of the two chaperonin molecules in the crystallographic asymmetric unit, which form different crystal contact patterns (Figure 4B). The apical domain in *Tth*-GroEL has high temperature factors as was observed in the *Ec*-GroEL structures (Braig et al., 1994; Xu et al., 1997); however, this cannot explain such a large deviation from 7-fold symmetry. Indeed, the conformational variety of the GroEL subunit in the *cis*-ring is much higher in the *Tth*-chaperonin complex (rmsd $\sim$2.7 Å) than that in the *Ec*-GroEL/ES complex (rmsd $\sim$0.2 Å) (Xu et al., 1997) or the uncomplexed *Ec*-GroEL structure (rmsd $\sim$0.5 Å) (Braig et al., 1994).

The *Tth*-GroEL subunits in the *cis*-ring can be roughly classified into two types (type I and type II) according to the degree of twist of the apical domain against the intermediate domain due to the conformational flexibilities of the N and C terminus of the apical domain (Figure 4C). The apical domain of the type I subunit is more twisted into the *cis*-cavity. The conformation of the *Ec*-GroEL subunit is more similar to the type II conformation

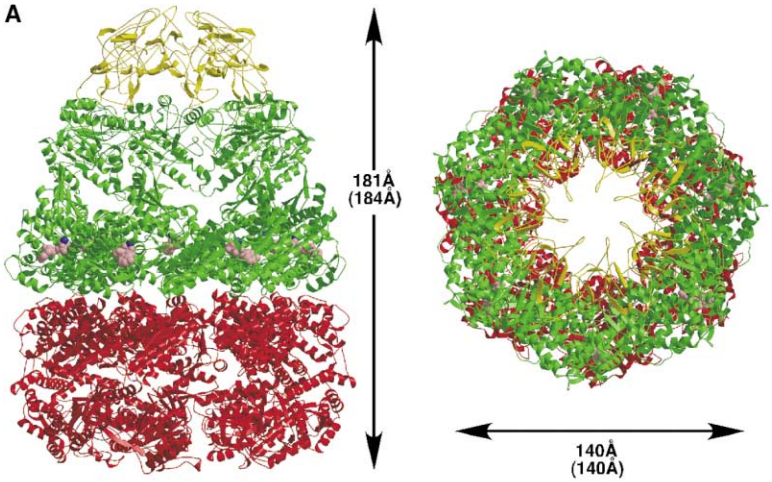

Figure 2. The Structure of the *Tth*-Chaperonin Complex

(A) The structure of the complex in a side (left) and top (right) view. The *trans*-ring, the *cis*-ring and GroES are colored red, green, and yellow, respectively. ADP molecules and Mg ions are shown as pink and orange, respectively. The sizes of the *Ec*-GroEL/ES complex (1AON) (Xu et al., 1997) are shown in parentheses.

(B) Locations of the nonconserved regions. A protomer is shown. Nonconserved regions (see Figure 3) are shown in red.

(C) The surface of the wall of the *cis*-cavity. Three subunits of both *Tth*-GroEL in the *cis*-ring and *Tth*-GroES are shown. Electrostatic potentials were calculated with the program GRASP (Honig and Nicholls, 1995). The polar surfaces are colored blue (positively charged) and red (negatively charged).

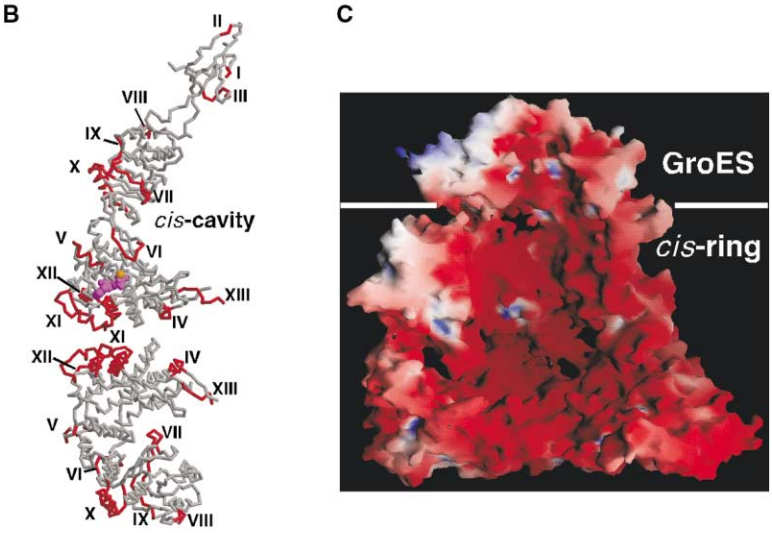

than type I. The *cis*-ring is, in principle, composed of three pairs of type I and type II subunits, and one type II subunit (Figure 4A). This means that every other subunit is twisted into the *cis*-cavity in the native *Tth*-chaperonin complex compared with the reconstituted *Ec*-GroEL/ES complex. The interface of the GroEL subunits is adjusted by residues 296–317 (Figure 4C). Residues 296–317, and the N and C termini of the apical domain both contain several conserved glycine residues (Gly191, Gly296, Gly297, Gly305, Gly317, Gly373, and Gly374) (Figure 3).

The large asymmetry observed in the *cis*-ring of the *Tth*-chaperonin complex suggests that positive cooperativity of the upward movement of the intermediate and apical domains is not strong enough to maintain 7-fold symmetry. However, the observed ring structure seems quite stable because the two molecules in the crystallographic asymmetric unit show the same pattern of distortion. It is possible that a ring structure with perfect 7-fold symmetry, as observed in *Ec*-GroEL/ES complex, and the distorted ring structures observed in *Tth*-chaperonin complex are in equilibrium; possible mechanisms of transition are discussed below.

Positive Cooperativity

Positive cooperativity in ATP binding and the associated conformational change observed in the GroEL subunits are essential for the binding of GroES and facilitates the catalytic cycle of chaperonin (Sigler et al., 1998; Thirumalai and Lorimer, 2001). It has been proposed that the signal is transmitted through both rings in the *Ec*-GroEL$_{14}$ complex, but only through the *trans*-ring in the *Ec*-GroEL/ES complex (Yifrach and Horovitz, 1995; Inbar and Horovitz, 1997). It seems that a specific intersubunit salt bridge between Glu386 and Arg197 plays a major role in the cooperativity (Ma et al., 2000; Ranson et al., 2001; Yifrach and Horovitz, 1994). Indeed, the *Ec*-GroEL R197A mutant showed significantly reduced cooperativity in ATP hydrolysis (Yifrach and Horovitz, 1994). A cryo-EM study suggested that this Glu386 exchanges the salt bridge partner from Arg197 in the apical domain to Lys80 in the equatorial domain upon ATP binding (Ranson et al., 2001). ATP binding induces the conformational change of the intermediate domain that contains Glu386, and also Asp398, a residue essential for hydrolysis of ATP (Rye et al., 1997; Xu et al., 1997); this switch of the intersubunit salt bridges was proposed

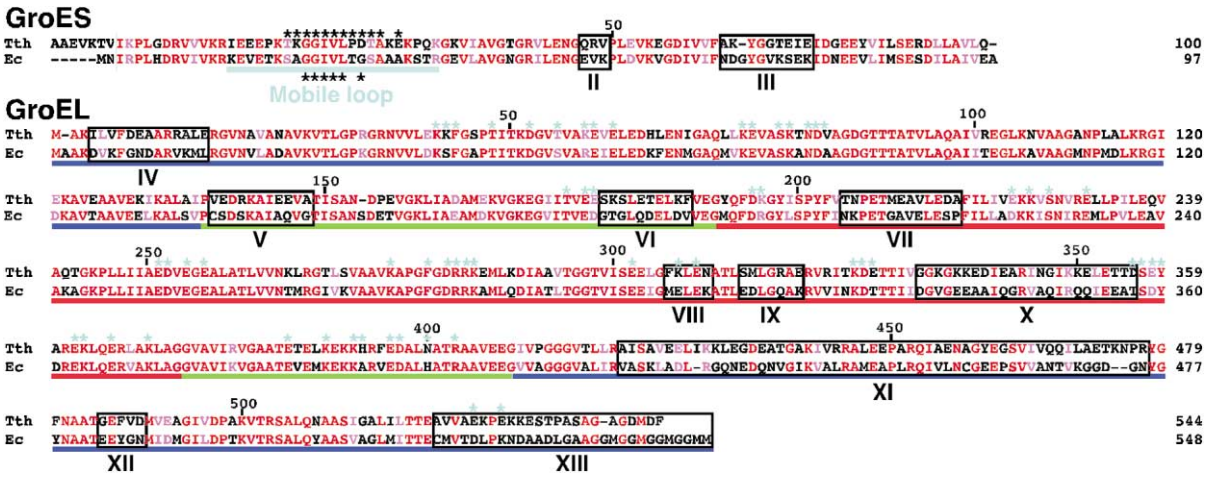

Figure 3. Sequence Alignment of *T. thermophilus* Chaperonin and *E. coli* Chaperonin

The equatorial, intermediate, and apical domains are underlined with blue, green and red lines. Identical and similar residues are shown in red and pink, respectively. Nonconserved regions are shown in boxes I–XIII. Residues facing the *cis*-cavity are indicated with cyan stars. Black stars indicate residues in the mobile loop interacting with GroEL.

to be a signal for positive cooperativity (Ranson et al., 2001; White et al., 1997). Recently, Danziger et al. suggested that an intrasubunit salt bridge between Asp155 and Arg395 in *Ec*-GroEL is important for stabilizing the intersubunit salt bridge between Glu386 and Arg197 because the *Ec*-GroEL D155A mutant shows an ATP-induced break in the intraring symmetry (Danziger et al., 2003).

Surprisingly, the *Tth*-chaperonin complex lacks both these salt bridges between the equivalent residues Glu385 and Lys196, and Asp154 and Arg394 in the *trans*-ring (Figure 5). Instead, Arg394 forms an intrasubunit salt bridge with Glu390. This is due to conformational differences at the N termini of helix G containing Asp154, and helix M containing Glu385, Glu390, and Arg394 in the intermediate domain (Figure 5). A 1 residue deletion before Asp154 in *Tth*-GroEL affects the conformation of the N terminus of helix G (Figure 3). The distances between Glu385 and Lys196 and between Asp154 and Arg394 are ~5.5 and ~4.7 Å, respectively. Considering the average coordinate error at this resolution (~0.5 Å), it seems unlikely these residues interact. These results suggest that the intersubunit salt bridge between Glu385 and Lys196 may not be essential for signaling of positive cooperativity in the *Tth*-chaperonin complex.

Peptide Binding Site, Helices H and I

Helices H and I of the GroEL apical domain bind substrate protein in the *trans*-ring and the GroES mobile loop in the *cis*-ring mainly by hydrophobic interactions (Buckle et al., 1997; Chen and Sigler, 1999; Xu et al., 1997). These helices are known to be flexible particularly at the C termini (Ashcroft et al., 2002; Chen and Sigler, 1999) and are thought to adjust their conformation in response to the bound peptide (Chen and Sigler, 1999). Such conformational plasticity is suggested to account for the ability of GroEL to bind a wide range of sequences and structures (Chen and Sigler, 1999). In the *Ec*-GroEL/ES complex structure, the C terminus of helix I is unfolded (but ordered) in the *trans*-ring but folded in the *cis*-ring, and the conformations of these helices are different (rmsd 1.7 Å) between the *cis*- and *trans*-rings (i.e., with and without bound GroES mobile loop). In contrast, in the *Tth*-chaperonin complex, these helices are folded in both rings: this is the case for the structure of the isolated apical domain (minichaperone) from *T. thermophilus* (Hua et al., 2001). Consequently, the conformation of these helices of the *cis*- and *trans*-ring and of the minichaperone are very similar and superimpose with an rmsd of 0.3 Å (Figure 6). This result strongly suggests that they are less flexible than those in the *Ec*-GroEL/ES complex despite the broad substrate specificity as discussed in the previous section. Indeed, replacement of residues around helices H and I of *Ec*-GroEL by those of *Tth*-GroEL are known to increase the stability of the apical domain by improving hydrophobic packing, and optimizing hydrogen bonding and structural rearrangement (Wang et al., 1999). As a result, the groove between helices H and I of *Tth*-GroEL seems more hydrophobic than that of *Ec*-GroEL. Indeed, in the *Tth*-GroEL minichaperone structure solved at 1.78 Å (Hua et al., 2001), there are no corresponding water molecules found in an *Ec*-GroEL minichaperone structure (Ashcroft et al., 2002). These results indicate that *Tth*-GroEL forms stronger hydrophobic interactions with the substrate protein than *Ec*-GroEL. Then, we measured binding kinetics of *Tth*-GroEL for reduced α-lactalbumin at 25°C using the surface plasmon resonance (BIAcore) (Table 2). As expected, *Tth*-GroEL exhibited slower dissociation rate (k_{off}) and lower dissociation constant (K_D) for reduced α-lactalbumin than *Ec*-GroEL (Murai et al., 1995). The affinity would be higher at the physiological temperature of *T. thermophilus* (~80°C), as hydrophobic interactions become stronger as temperature increases. These results suggest the highly hydrophobic nature of the groove of *Tth*-GroEL may compensate for the lack of plasticity of these helices upon the substrate binding. The structure of the *Tth*-GroEL minichaperone is thermostable (*Tm* > 100°C) and

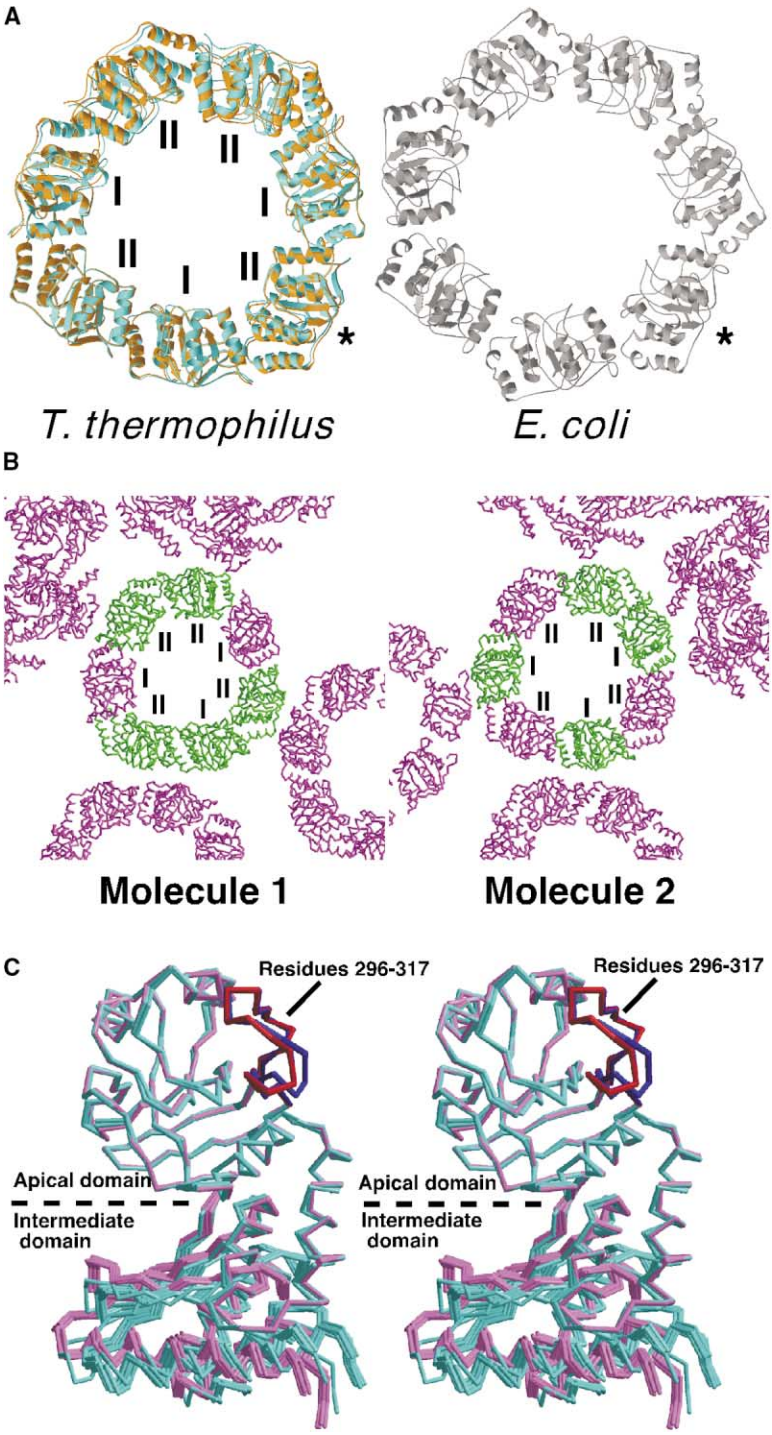

Figure 4. The Structure of the *cis*-Ring

(A) The conformation of the *cis*-ring around the apical domains of *Tth*-GroEL (left) and *Ec*-GroEL (right) viewed from the top. The subunits indicated by stars were used for the superposition. The two *Tth*-chaperonin complex molecules in an asymmetric unit are overlapped as colored blue and orange. The types of *Tth*-GroEL subunits are indicated inside the ring as I and II.

(B) Crystal packing of the two molecules in the asymmetric unit around the apical domains viewed from the top. In each molecule, different subunits are involved in the crystal contacts (green). The types of the *Tth*-GroEL subunits are indicated inside the ring as I and II. The number and the disposition of the subunits involved in the contacts are different between the two molecules in the asymmetric unit: one type I and four type II subunits in one molecule (left), and three type I and one type II subunits in the other molecule (right).

(C) Stereoview of the various conformations of *Tth*-GroEL subunits in the *cis*-ring. Only the apical and intermediate domains are shown. Fourteen *Tth*-GroEL subunits in an asymmetric unit are superimposed. The type I and II conformations of *Tth*-GroEL are colored cyan and pink, respectively. Residues 296–317 of the type I and II are colored blue and red, respectively.

no significant secondary structural change was detected up to *Tm* (Hua et al., 2001). Therefore, it is likely that helices H and I stay folded at the physiological temperature of *T. thermophilus*.

Mobile Loop

GroES binds to GroEL via a mobile loop that is disordered in uncomplexed GroES structure (Hunt et al., 1996), but ordered upon binding with GroEL (Xu et al., 1997). In the *Tth*-chaperonin complex structure, the overall shape of *Tth*-GroES has an approximate 7-fold symmetry, while the *cis*-ring rim of *Tth*-GroEL deviates from the molecule's 7-fold symmetry. However, all seven *Tth*-GroES subunits are involved in the interactions with *Tth*-GroEL. In order to maintain the contacts with the *Tth*-GroEL *cis*-ring, *Tth*-GroES changes the conformation of the mobile loop slightly between subunits (rmsd ~0.6 Å). This suggests the affinity of *Tth*-GroES for *Tth*-GroEL

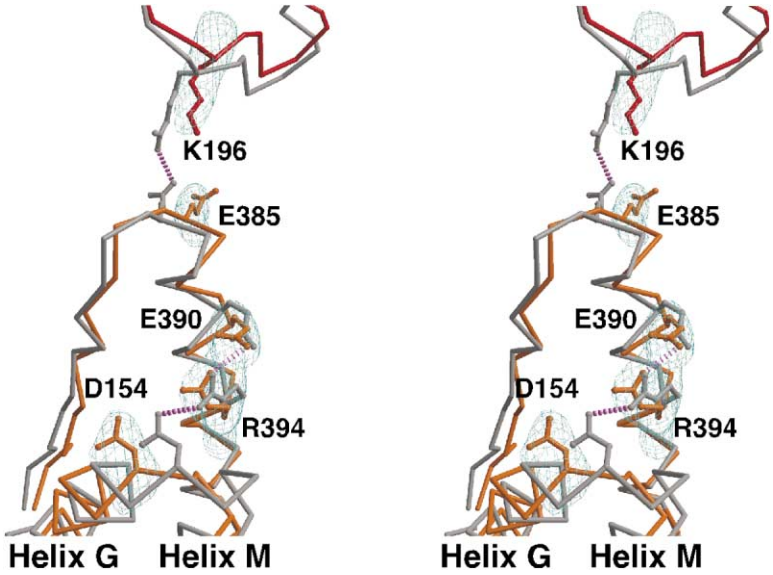

Figure 5. Stereoview of the Residues around the Intermediate Domain in the *trans*-Ring

A $F_o - F_c$ omit map, which is calculated after removing the labeled residues from the model, are shown in blue (contoured at 3σ). Two adjacent *Tth*-GroEL subunits (red and orange) are shown. *Ec*-GroEL (gray) are overlapped. The residue names are of *Tth*-GroEL. Lys196 belongs to the apical domain, while the others to the intermediate domain. The hydrogen bonds are shown as a pink dotted line.

differs between subunits. In contrast, the mobile loop of *Ec*-GroES shows no conformational variation in the *Ec*-GroEL/ES complex (rmsd ~0.2 Å).

The mobile loop of *Tth*-GroES (residues 19–42) and *Ec*-GroES (residues 14–37) show high sequence homology (58.3%) (Figure 3) with a conserved GGIVL sequence that interacts with helices H and I of *Ec*-GroEL (Xu et al., 1997). Despite these similarities, the *Tth*-GroES and *Ec*-GroES mobile loops show significantly different conformations (Figure 7). Moreover, *Tth*-GroES contacts with residues 305–310 in the adjacent *Tth*-GroEL subunit as well as helices H and I, while *Ec*-GroES interacts only with helices H and I of *Ec*-GroEL (Figure 7). Pro33, Asp34, and Thr35 on the mobile loop and Gly305, Lys307, and Asn310 in *Tth*-GroEL are involved in this interaction, although exact interaction patterns (van der Waals interactions and hydrogen bonds) between these residues varies from subunit to subunit because of the asymmetry of the *cis*-ring. This suggests the affinity to GroEL could be higher in *Tth*-GroES than *Ec*-GroES. This could explain why the native *Tth*-chaperonin complex can be purified, whereas the *Ec*-GroEL/ES complex dissociates during purification. However, residues 305–310 in the *Ec*-GroEL/ES complex may interact with *Ec*-GroES during the functional ATPase cycle, considering an *Ec*-GroEL mutant L309K increased the rate of *Ec*-GroES exchange and was unable to rescue GroEL-deficient *E. coli* cells (Fenton et al., 1994).

Residues 305–310 in *Tth*-GroEL may not be involved in substrate binding, since these residues are located outside the central cavity in the *trans*-ring (region VIII in Figure 2B). This suggests *Tth*-GroES could bind to the *Tth*-GroEL *cis*-ring together with substrate proteins. There has been some debate whether substrate proteins bound to helices H and I are displaced into the *cis*-cavity prior to the GroES binding to the GroEL *cis*-ring (Chen and Sigler, 1999; Cliff et al., 1999; Kawata et al., 1999). The existence of the additional binding site on GroEL exclusively for GroES suggests that substrate proteins could be displaced after GroES binding.

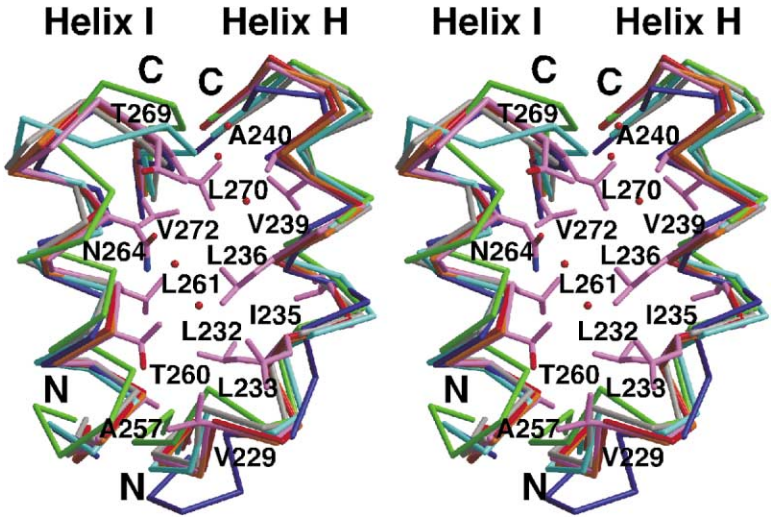

Figure 6. Stereoview of the Superposition of Helices H and I in the Various Structures of *Tth*-GroEL and *Ec*-GroEL

Helices H and I in the *cis*-ring (pink) and the *trans*-ring (red) of the *Tth*-chaperonin complex, the *cis*-ring (blue) and the *trans*-ring (cyan) of the *Ec*-GroEL/ES complex (PDB entry 1AON) (Xu et al., 1997), in $Ec\text{-GroEL}_{14}$ (1OEL) (Braig et al., 1995) (green) and the minichaperone of *Tth*-GroEL (1SRV) (Hua et al., 2001) (orange) and *Ec*-GroEL (1LA1) (Ashcroft et al., 2002) (gray) are shown. The side chain of the residues in the *cis*-ring of the *Tth*-chaperonin complex are shown. Water molecules found in a minichaperone structure of *Ec*-GroEL (1LA1) are shown in red.

Table 2. Binding Kinetics of the Interaction between GroEL and Immobilized Reduced α-Lactalbumin

	k_{on} (10^5 M^{-1} s^{-1})	k_{off} (10^{-4} s^{-1})	K_D (10^{-9} M)
Tth-GroEL	1.53	0.97	0.63
Ec-GroEL	1.96[a]	2.08[a]	1.03[a]

[a] Taken from the values in Murai et al. (1995).

Deviation from the 7-Fold Symmetry and Substrate Proteins

Unexpectedly, the *Tth*-chaperonin complex structure has a large deviation from the 7-fold symmetry around the rim of the *cis*-ring (Figure 4A). In the *Ec*-GroEL D155A mutant, a deviation from the 7-fold symmetry was observed when a nonsaturating ATP concentration of 5 μM was present, which disappeared when ATP was absent or at a saturating concentration (100 μM) (Danziger et al., 2003). The authors suggested that the absence of an intrasubunit salt bridge between Asp155 and Arg395 weakened the intersubunit salt bridge between Arg197 and Glu386, which would free the apical domains and thus create the break in the 7-fold symmetry in the ring. Considering the lack of these two salt bridges, *Tth*-GroEL seems to have more flexible apical domains and weaker positive cooperativity than *Ec*-GroEL, thereby enabling the *Tth*-GroEL ring to deviate from the 7-fold symmetry. However, considering the highly conserved nature of amino acids in both *Tth*-GroEL and *Ec*-GroEL, in particular glycine residues in the N and C terminus of the apical domain and residues 296–317, and the high flexibility of residues 301–310 in *Ec*-GroEL (Chen and Sigler, 1999), the *Ec*-GroEL *cis*-ring may exhibit a large deviation from the 7-fold symmetry under certain circumstances.

Interestingly, the asymmetric ring of the *Ec*-GroEL D155A mutant at the nonsaturating ATP concentration is composed of three subunits in one conformation and four subunits in another (Danziger et al., 2003), as observed in the *cis*-ring of the *Tth*-chaperonin complex. The three subunits with similar conformation are adjacent to each other, and were suggested to correspond to the relaxed (*r*) conformation with high affinity for ATP, with the remaining four subunits adopting the tense (*t*) conformation with low affinity for ATP. Thus, the D155A mutation was proposed to convert the allosteric transition from concerted to sequential. In the asymmetric *cis*-ring of the *Tth*-chaperonin complex, the arrangement of the subunits are different from those observed in the *Ec*-GroEL D155A mutant; the subunits with similar conformation are not adjacent to each other. Moreover, all subunits in the *cis*-ring of *Tth*-GroEL bind ADP at the ATP/ADP binding site. These results strongly suggest that the large deviation from the 7-fold symmetry around the rim of the *cis*-ring is probably not caused by the conversion of the allosteric transition from concerted to sequential as suggested by Danziger et al. (2003) for *Ec*-GroEL.

The cause of this large deviation from the 7-fold symmetry is unclear. However, there are several pieces of evidences suggesting that substrate peptides may cause an asymmetry in the GroEL ring. Substrate proteins are known to bind typically to three consecutive GroEL subunits (Farr et al., 2000) and to be unfolded from the misfolded condition by stretching during upward rigid-body movement of the apical domains (Shtilerman et al., 1999). These facts suggest that the subunit bound to substrate proteins may behave differently from the substrate-free subunits during apical domain movement induced upon ATP binding, considering the flexibility and the weak positive cooperativity in *Tth*-GroEL as suggested above. Moreover, the (*Ec*-GroEL-peptide)$_{14}$ structure revealed that peptide binding induces rotation of apical domains (Wang and Chen, 2003). The authors of this study suggested that a highly asymmetric ring structure could be formed in a situation where a single substrate peptide binds to one ring as proposed in vivo. Considering these facts, the large deviation from the 7-fold symmetry around the *cis*-ring rim in the *Tth*-chaperonin complex could be caused by substrate peptides during the upward movement of the apical domains. Under this asymmetric environment, the observed deviated configuration (three pairs of type I and type II, plus type II), where a dimer of type I and II subunits forms a

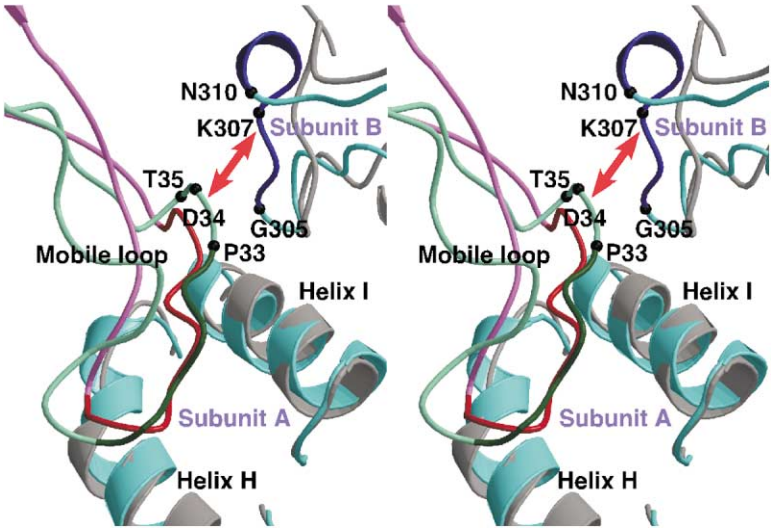

Figure 7. Stereoview of the *Tth*-Chaperonin Complex and the *Ec*-GroEL/ES Complex around the Mobile Loop of GroES

Tth-GroEL (cyan), *Ec*-GroEL (gray), *Tth*-GroES (light green), and *Ec*-GroES (pink) are shown. The conserved motif GGIVL in *Tth*-GroES and *Ec*-GroES are shown in dark green and red, respectively. Residues 305–310 of *Tth*-GroEL are shown in blue. The Cα atoms of the residues involved in the unique contacts found in the *Tth*-chaperonin complex are shown. The unique interaction found in the *Tth*-chaperonin complex is shown as a orange arrow.

stable unit, seems to be a more preferable arrangement than the ring with perfect 7-fold symmetry. Thus, the asymmetric *Tth*-chaperonin structure is likely to represent the true conformation of the GroEL/ES complex during enzymatic turnover. It is very important to study if the *Ec*-GroEL/ES complex shows any asymmetry during turnover with substrate proteins, particularly using electron microscopic single-particle analysis, recently applied for the *Ec*-GroEL D155A mutant (Danziger et al., 2003).

Experimental Procedures

Purification and Crystallization

The native *Tth*-chaperonin complex was purified from intact *T. thermophilus* HB8, and crystallized as previously described (Shimamura et al., 2003).

Identification of Substrate Proteins

One-dimensional SDS-PAGE was performed according to standard protocols. Protein spots were excised from the gel, washed, in-gel reduced, *S*-alkylated, and in-gel digested with trypsin (Promega) as previously described (Shevchenko et al., 1996). The peptides eluted from the gel pieces were desalted on a $ZipTip_{C18}$ column (Millipore), eluted with 50% acetonitrile containing α-cyano-4-hydroxycinnamic acid (5 mg/ml) and 0.1% trifluoroacetic acid, and analyzed by MALDI-TOF mass spectrometry (Axima CFR, Shimadzu). Calibration of mass spectra was typically performed using trypsin autodigestion peaks as internal standards. Peptide fingerprint searches were performed using the program PeptideSearch kindly provided by Dr. Saravanan Ponnusamy, searching a database of *T. thermophilus* genome sequences. Some of the major peaks were subjected to further MS/MS analysis using the PSD (post source decay) mode of the Axima CFR to determine possible amino acid sequences. For N-terminal amino acid sequencing, proteins were transferred onto a polyvinylidene difluoride membrane (Bio-rad) and analyzed with a gas phase peptide sequencer (PPSQ-21, Shimadzu).

Structure Determination and Refinement

Data collection from crystals of the *Tth*-chaperonin complex was performed as described (Shimamura et al., 2003). Molecular replacement was performed with the program AMoRe (Navaza, 1994) using the structure of the *Ec*-GroEL/ES complex (Xu et al., 1997) as a search model. Refinement and model building were performed with the programs CNS (Brunger et al., 1998) and O (Jones et al., 1991). All refinements were carried out at 2.8–40 Å resolution using all reflections. 3% of the data were used for cross validation. Noncrystallographic symmetry (NCS) constraints were used at the early stages of refinement. Once R_{work} and R_{free} factors reached ~34%, where no further significant decrease of the R values were observed, NCS restraints instead of constraints were used for refinement. As was used in the refined *Ec*-$GroEL_{14}$ structure (Braig et al., 1995), the different domains were allocated different weights of the NCS restraints which were optimized to give the lowest R_{free} value. The equatorial and intermediate domains were more tightly restrained, and the apical domain with *Tth*-GroES allowed more generous deviations. At the initial refinement stages, type I and II subunits in the apical domain of the *cis*-ring were grouped in the same NCS restraint group but were grouped differently at the final stages. The electron density was clear in most regions, except the C-terminal 13–17 residues of *Tth*-GroEL and the N-terminal 4 or 5 residues of *Tth*-GroES depending on the subunit. These residues are not included in the current model. The final model contains seven ADP molecules, seven Mg^{2+} ions, and seven DMSO molecules per chaperonin molecule. Data collection and refinement statistics are shown in Table 1. The calculation of the rmsd was performed using the program LSQKAB (CCP4, 1994). Figures were prepared using BobScript (Esnouf, 1997) and Raster3D (Merritt and Bacon, 1997).

Binding Kinetics for Reduced α-Lactalbumin

The reduced α-lactalbumin was immobilized as described (Murai et al., 1995). The buffer used for the flow (free buffer) was 10 mM HEPES (pH 7.4) containing 150 mM KCl, 20 mM $MgCl_2$, and 2 mM dithiothreitol. Samples were injected at 25°C with a flow rate of 5 μl/min onto the sensor chip surface on which α-lactalbumin had been immobilized. The traces of the association and dissociation process were analyzed as described except that 10 mM glycine-HCl buffer (pH 3.0) was used in the dissociation phase (Murai et al., 1995). The dissociation constant (K_D) was calculated from the equation $K_D = k_{off}/k_{on}$.

Acknowledgments

Drs. H. Matsuno and Y. Okahata are acknowledged for the use of MALDI-TOF mass spectrometry. We thank Drs. S. Takada and F. Takagi for their discussion on the chaperonin substrate protein, Dr. E. Mitchell at ESRF ID14 for technical assistance, and Drs. T. Iverson and B. Byrne for critically reading the manuscript. This work was supported by a grant from the National Project on Protein Structural and Functional Analyses from the Ministry of Education, Culture, Sports, Science, and Technology.

Received: February 27, 2004
Revised: May 5, 2004
Accepted: May 18, 2004
Published: August 10, 2004

References

Aoki, K., Motojima, F., Taguchi, H., Yomo, T., and Yoshida, M. (2000). GroEL binds artificial proteins with random sequences. J. Biol. Chem. *275*, 13755–13758.

Ashcroft, A.E., Brinker, A., Coyle, J.E., Weber, F., Kaiser, M., Moroder, L., Parsons, M.R., Jager, J., Hartl, U.F., Hayer-Hartl, M., et al. (2002). Structural plasticity and noncovalent substrate binding in the GroEL apical domain. A study using electrospray ionization mass spectrometry and fluorescence binding studies. J. Biol. Chem. *277*, 33115–33126.

Braig, K., Otwinowski, Z., Hegde, R., Boisvert, D.C., Joachimiak, A., Horwich, A.L., and Sigler, P.B. (1994). The crystal structure of the bacterial chaperonin GroEL at 2.8 Å. Nature *371*, 578–586.

Braig, K., Adams, P.D., and Brünger, A.T. (1995). Conformational variability in the refined structure of the chaperonin GroEL at 2.8Å resolution. Nat. Struct. Biol. *2*, 1083–1094.

Brinker, A., Pfeifer, G., Kerner, M.J., Naylor, D.J., Hartl, F.U., and Hayer-Hartl, M. (2001). Dual function of protein confinement in chaperonin-assisted protein folding. Cell *107*, 223–233.

Brunger, A.T., Adams, P.D., Clore, G.M., DeLano, W.L., Gros, P., Grosse-Kunstleve, R.W., Jiang, J.S., Kuszewski, J., Nilges, M., Pannu, N.S., et al. (1998). Crystallography & NMR system: a new software suite for macromolecular structure determination. Acta Crystallogr. D Biol. Crystallogr. *54*, 905–921.

Buckle, A.M., Zahn, R., and Fersht, A.R. (1997). A structural model for GroEL-polypeptide recognition. Proc. Natl. Acad. Sci. USA *94*, 3571–3575.

Bukau, B., and Horwich, A.L. (1998). The Hsp70 and Hsp60 chaperone machines. Cell *92*, 351–366.

CCP4 (Collaborative Computational Project, Number 4) (1994). The CCP4 suite: program for protein crystallography. Acta Crystallogr. D Biol. Crystallogr. *50*, 760–763.

Chaudhry, C., Farr, G.W., Todd, M.J., Rye, H.S., Brunger, A.T., Adams, P.D., Horwich, A.L., and Sigler, P.B. (2003). Role of the gamma-phosphate of ATP in triggering protein folding by GroEL-GroES: function, structure and energetics. EMBO J. *22*, 4877–4887.

Chen, L., and Sigler, P.B. (1999). The crystal structure of a GroEL/peptide complex: plasticity as a basis for substrate diversity. Cell *99*, 757–768.

Cliff, M.J., Kad, N.M., Hay, N., Lund, P.A., Webb, M.R., Burston, S.G., and Clarke, A.R. (1999). A kinetic analysis of the nucleotide-induced allosteric transitions of GroEL. J. Mol. Biol. *293*, 667–684.

Danziger, O., Rivenzon-Segal, D., Wolf, S.G., and Horovitz, A. (2003). Conversion of the allosteric transition of GroEL from concerted to

sequential by the single mutation Asp-155→Ala. Proc. Natl. Acad. Sci. USA *100*, 13797–13802.

Esnouf, R.M. (1997). An extensively modified version of MolScript that includes greatly enhanced coloring capabilities. J. Mol. Graph. Model. *15*, 132–134.

Farr, G.W., Furtak, K., Rowland, M.B., Ranson, N.A., Saibil, H.R., Kirchhausen, T., and Horwich, A.L. (2000). Multivalent binding of nonnative substrate proteins by the chaperonin GroEL. Cell *100*, 561–573.

Fenton, W.A., Kashi, Y., Furtak, K., and Horwich, A.L. (1994). Residues in chaperonin GroEL required for polypeptide binding and release. Nature *371*, 614–619.

Hartl, F.U., and Hayer-Hartl, M. (2002). Molecular chaperones in the cytosol: from nascent chain to folded protein. Science *295*, 1852–1858.

Honig, B., and Nicholls, A. (1995). Classical electrostatics in biology and chemistry. Science *268*, 1144–1149.

Houry, W.A., Frishman, D., Eckerskorn, C., Lottspeich, F., and Hartl, F.U. (1999). Identification of in vivo substrates of the chaperonin GroEL. Nature *402*, 147–154.

Hua, Q., Dementieva, I.S., Walsh, M.A., Hallenga, K., Weiss, M.A., and Joachimiak, A. (2001). A thermophilic mini-chaperonin contains a conserved polypeptide-binding surface: combined crystallographic and NMR studies of the GroEL apical domain with implications for substrate interactions. J. Mol. Biol. *306*, 513–525.

Hunt, J.F., Weaver, A.J., Landry, S.J., Gierasch, L., and Deisenhofer, J. (1996). The crystal structure of the GroES co-chaperonin at 2.8 Å resolution. Nature *379*, 37–45.

Inbar, E., and Horovitz, A. (1997). GroES promotes the T to R transition of the GroEL ring distal to GroES in the GroEL-GroES complex. Biochemistry *36*, 12276–12281.

Jones, T.A., Zou, J.Y., Cowan, S.W., and Kjeldgaard (1991). Improved methods for building protein models in electron density maps and the location of errors in these models. Acta Crystallogr. A *47* (*Pt 2*), 110–119.

Kawata, Y., Kawagoe, M., Hongo, K., Miyazaki, T., Higurashi, T., Mizobata, T., and Nagai, J. (1999). Functional communications between the apical and equatorial domains of GroEL through the intermediate domain. Biochemistry *38*, 15731–15740.

Ma, J., Sigler, P.B., Xu, Z., and Karplus, M. (2000). A dynamic model for the allosteric mechanism of GroEL. J. Mol. Biol. *302*, 303–313.

Mayhew, M., da Silva, A.C.R., Martin, J., Erdjument-Bromage, H., Tempst, P., and Hartl, F.U. (1996). Protein folding in the central cavity of the GroEL-GroES chaperonin complex. Nature *379*, 420–426.

Merritt, E.A., and Bacon, D.J. (1997). Raster3D: photorealistic molecular graphics. Methods Enzymol. *277*, 505–524.

Motojima, F., and Yoshida, M. (2003). Discrimination of ATP, ADP and AMPPNP by chaperonin GroEL; hexokinase treatment revealed the exclusive role of ATP. J. Biol. Chem. *278*, 26648–26654.

Murai, N., Taguchi, H., and Yoshida, M. (1995). Kinetic analysis of interactions between GroEL and reduced alpha lactalbumin. J. Biol. Chem. *270*, 19957–19963.

Navaza, J. (1994). AMoRe: an automated package for molecular replacement. Acta Crystallogr. A *50*, 157–163.

Ranson, N.A., Farr, G.W., Roseman, A.M., Gowen, B., Fenton, W.A., Horwich, A.L., and Saibil, H.R. (2001). ATP-bound states of GroEL captured by cryo-electron microscopy. Cell *107*, 869–879.

Rye, H.S., Burston, S.G., Fenton, W.A., Beechem, J.M., Xu, Z., Sigler, P.B., and Horwich, A.L. (1997). Distinct actions of *cis* and *trans* ATP within the double ring of the chaperonin GroEL. Nature *388*, 792–798.

Rye, H.S., Roseman, A.M., Chen, S., Furtak, K., Fenton, W.A., Saibil, H.R., and Horwich, A.L. (1999). GroEL-GroES cycling: ATP and nonnative polypeptide direct alternation of folding-active rings. Cell *97*, 325–338.

Sakikawa, C., Taguchi, H., Makino, Y., and Yoshida, M. (1999). On the maximum size of proteins to stay and fold in the cavity of GroEL underneath GroES. J. Biol. Chem. *274*, 21251–21256.

Shevchenko, A., Wilm, M., Vorm, O., and Mann, M. (1996). Mass spectrometric sequencing of proteins silver-stained polyacrylamide gels. Anal. Chem. *68*, 850–858.

Shimamura, T., Koike-Takeshita, A., Yokoyama, K., Yoshida, M., Taguchi, H., and Iwata, S. (2003). Crystallization of the chaperonin GroEL-GroES complex from Thermus thermophilus HB8. Acta Crystallogr. D Biol. Crystallogr. *59*, 1632–1634.

Shtilerman, M., Lorimer, G.H., and Englander, S.W. (1999). Chaperonin function: folding by forced unfolding. Science *284*, 822–825.

Sigler, P.B., Xu, Z., Rye, H.S., Burston, S.G., Fenton, W.A., and Horwich, A.L. (1998). Structure and function in GroEL-mediated protein folding. Annu. Rev. Biochem. *67*, 581–608.

Taguchi, H., and Yoshida, M. (1998). Chaperonin from thermophile Thermus thermophilus. Methods Enzymol. *290*, 169–180.

Taguchi, H., Konishi, J., Ishii, N., and Yoshida, M. (1991). A chaperonin from a thermophilic bacterium, *Thermus thermophilus*, that controls refolding of several thermophilic enzymes. J. Biol. Chem. *266*, 22411–22418.

Taguchi, H., Ueno, T., Tadakuma, H., Yoshida, M., and Funatsu, T. (2001). Single-molecule observation of protein-protein interactions in the chaperonin system. Nat. Biotechnol. *19*, 861–865.

Thirumalai, D., and Lorimer, G.H. (2001). Chaperonin-mediated protein folding. Annu. Rev. Biophys. Biomol. Struct. *30*, 245–269.

Viitanen, P.V., Gatenby, A.A., and Lorimer, G.H. (1992). Purified GroEL interacts with the non-native states of a multitude of E. coli proteins. Protein Sci. *1*, 361–369.

Wang, J., and Chen, L. (2003). Domain motions in GroEL upon binding of an oligopeptide. J. Mol. Biol. *334*, 489–499.

Wang, J.D., Herman, C., Tipton, K.A., Gross, C.A., and Weissman, J.S. (2002). Directed evolution of substrate-optimized GroEL/S chaperonins. Cell *111*, 1027–1039.

Wang, Q., Buckle, A.M., Foster, N.W., Johnson, C.M., and Fersht, A.R. (1999). Design of highly stable functional GroEL minichaperones. Protein Sci. *8*, 2186–2193.

Weissman, J.S., Hohl, C.M., Kovalenko, O., Kashi, Y., Chen, S., Braig, K., Saibil, H.R., Fenton, W.A., and Horwich, A.L. (1995). Mechanism of GroEL action: productive release of polypeptide from a sequestered position under GroES. Cell *83*, 577–587.

White, H.E., Chen, S., Roseman, A.M., Yifrach, O., Horovitz, A., and Saibil, H.R. (1997). Structural basis of allosteric changes in the GroEL mutant Arg197→Ala. Nat. Struct. Biol. *4*, 690–694.

Xu, Z., Horwich, A.L., and Sigler, P.B. (1997). The crystal structure of the asymmetric GroEL-GroES-(ADP)7 chaperonin complex. Nature *388*, 741–750.

Yifrach, O., and Horovitz, A. (1994). Two lines of allosteric communication in the oligomeric chaperonin GroEL are revealed by the single mutation Arg196→Ala. J. Mol. Biol. *243*, 397–401.

Yifrach, O., and Horovitz, A. (1995). Nested cooperativity in the ATPase activity of the oligomeric chaperonin GroEL. Biochemistry *34*, 5303–5308.

Yifrach, O., and Horovitz, A. (1996). Allosteric control by ATP of nonfolded protein binding to GroEL. J. Mol. Biol. *255*, 356–361.

Accession Numbers

The atomic coordinates and the structure factor (PDB codes 1WE3 and 1WF4) have been deposited in the Protein Data Bank, Research Collaboratory for Structural Bioinformatics.